

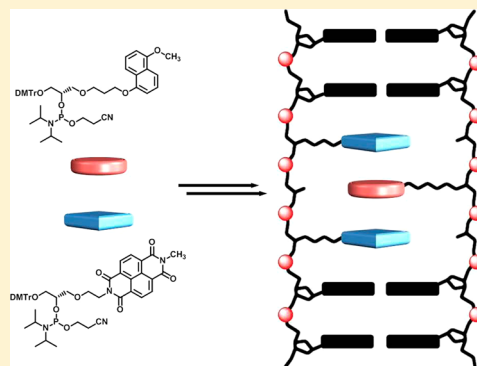
NDI and DAN DNA: Nucleic Acid-Directed Assembly of NDI and DAN

Brian A. Ikkanda, Stevan A. Samuel, and Brent L. Iverson*

Department of Chemistry, The University of Texas at Austin, Austin, Texas 78712, United States

S Supporting Information

ABSTRACT: Two novel DNA base surrogate phosphoramidites **1** and **2**, based upon relatively electron-rich 1,5-dialkoxynaphthalene (DAN) and relatively electron-deficient 1,4,5,8-naphthalenetetracarboxylic diimide (NDI), respectively, were designed, synthesized, and incorporated into DNA oligonucleotide strands. The DAN and NDI artificial DNA bases were inserted within a three-base-pair region within the interior of a 12-mer oligonucleotide duplex in various sequential arrangements and investigated with CD spectroscopy and UV melting curve analysis. The CD spectra of the modified duplexes indicated B-form DNA topology. Melting curve analyses revealed trends in DNA duplex stability that correlate with the known association of DAN and NDI moieties in aqueous solution as well as the known favorable interactions between NDI and natural DNA base pairs. This demonstrates that DNA duplex stability and specificity can be driven by the electrostatic complementarity between DAN and NDI. In the most favorable case, an NDI–DAN–NDI arrangement in the middle of the DNA duplex was found to be approximately as stabilizing as three A–T base pairs.



INTRODUCTION

The DNA double helix is a molecular architecture endowed with numerous properties that enable it to serve as an ideal scaffold for precise arrangement of aromatic moieties.^{1–3} Non-covalent interactions between aromatic nucleobases, combined with desolvation effects, contribute to the DNA duplex structure, specificity, and stability.^{4,5} In particular, the remarkable specificity of complementary oligonucleotide strands derived from Watson–Crick hydrogen bonding can be exploited to arrange various non-natural DNA base surrogates in a highly predictable fashion. Because base pairs are stacked in a ladderlike fashion, properties such as fluorescence⁶ and electron transfer^{7,8} as well as various complex supramolecular architectures⁹ can be investigated. The advanced nature of automated DNA synthesis greatly simplifies the placement of novel DNA base surrogates in a strand at any chosen location(s) within a sequence.

Several non-natural DNA base surrogates based on moieties with particular structure and function have been designed and synthesized that alter DNA stability and structure,^{10–13} including efforts to expand the genetic code with designed nucleobases.^{14–17} Through these studies, a great deal has been learned about requirements for successful DNA duplex formation in the presence of non-natural aromatic moieties. For example, designed nucleobases with alternative patterns of hydrogen bonding have been successfully incorporated into DNA duplexes, demonstrating that the hydrogen-bonding pattern found in natural DNA bases can be altered and still produce stable duplexes.^{18,19} Non-hydrogen-bonding yet isosteric DNA bases^{20,21} as well as other non-natural aromatic

units that promote zipperlike, stacked assembly²² have also been used in the design of artificial DNA structures.

We^{23–25} and others^{26,27} have been exploring the use of relatively electron-rich 1,5-dialkoxynaphthalene (DAN) and relatively electron-deficient 1,4,5,8-naphthalenetetracarboxylic diimide (NDI) (Figure 1) derivatives in aqueous solution to create novel folded and assembled structures based on alternating face-centered stacking of the DAN and NDI units.²³ Importantly, in strongly interacting solvents such as water, NDI and DAN have an association constant that is 1 or 2 orders of magnitude larger than the self-association constant of either NDI or DAN, respectively.²⁸ This specificity is thought to be due to complementary electrostatic interactions that can best be rationalized by focusing on the local and direct interactions of the highly polarized substituents (i.e., the diimide carbonyl groups of NDI and the ether oxygen atoms of DAN) on the periphery of the aromatic rings.²⁹ Such considerations explain why DAN and NDI adopt a fully face-centered stacking geometry in the solid state (Figure 2a) while NDI self-stacks in an offset mode (Figure 2b) and DAN does not prefer to self-stack but rather adopts a herringbone geometry in the solid state (Figure 2c).³⁰ In the context of desolvation, these preferred electrostatic-driven geometries would favor DAN–NDI association over NDI or DAN self-association in water. Interestingly, in previous work involving duplex assembly from relatively flexible amide-linked chains of DAN and NDI units,²⁵ the free energy of duplex formation

Received: December 5, 2013

Published: February 6, 2014

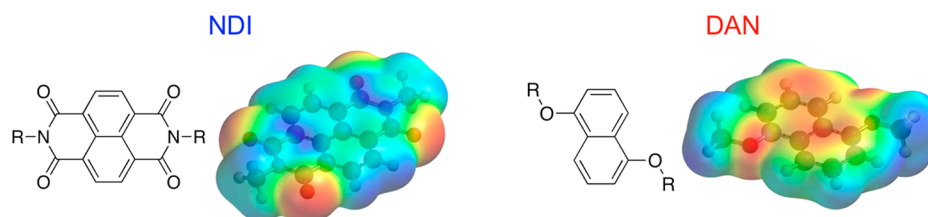


Figure 1. Structures and electrostatic potential surfaces calculated for (left) NDI and (right) DAN using DFT (B3LYP/6-31G*) as implemented in Spartan (Wavefunction, Inc.).

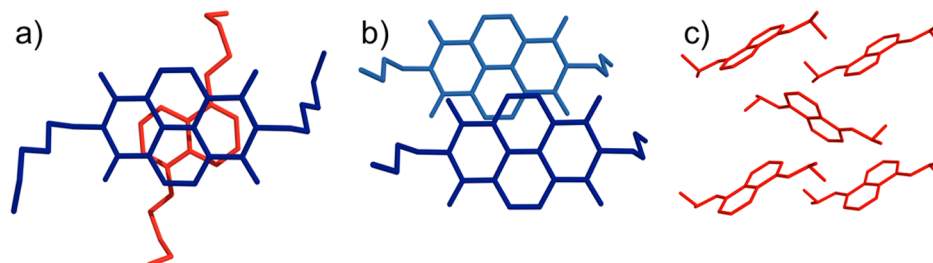


Figure 2. X-ray crystal structures of (a) DAN–NDI face-centered stacked monomers,³² (b) NDI–NDI offset stacked monomers,³³ and (c) DAN herringbone geometry in the solid state.³³

decreased only slightly as the temperature increased, demonstrating an apparent enthalpy–entropy compensation effect.³¹

Herein is described the synthesis of novel DAN and NDI DNA base surrogate phosphoramidites and their incorporation into DNA oligonucleotides. The stabilities and structures of various DAN- and NDI-modified oligomers were investigated. Complementary oligonucleotides that assembled to allow for alternating NDI–DAN–NDI stacking proved to be more stable than any of the other combinations investigated, demonstrating, to the best of our knowledge, for the first time that a stacking preference based on electrostatic complementarity can drive duplex stability and specificity.

RESULTS

Design of Modified Phosphoramidites. The NDI and DAN building blocks **1** and **2** were specifically designed to provide the appropriate flexibility and spacing needed to align NDI and DAN units in a face-centered stack at the center of the DNA duplex structure (Figure 3). Both **1** and **2** utilize the simplified (*S*)-GNA backbone (Figure 4), which is known to promote interstrand stacking, leading to relatively stable duplexes.³⁴ The (*S*)-GNA backbone was used instead of its enantiomeric analogue particularly because of its known double-helical structure based on X-ray crystallographic studies, which may help explain the modified duplex melting temperature.^{35,36} On the basis of qualitative computer models (Figure 3), linkers of two methylene units for NDI and three methylene units for DAN appeared to be optimum. These linker lengths were judged to be long enough to allow exactly the same face-centered stacking geometry seen in previous foldamers in aqueous solution^{23,24} as well as in alternating stacks observed in the solid state.^{32,33} It should be noted that rather than base pairing per se, the DAN and NDI units are intended to stack in more of a zipper-type arrangement, reminiscent of the systems reported by Leumann and co-workers.²² The unique aspect of the present approach is the well-documented preference for alternating stacking between DAN and NDI units, adding a new specificity element to the duplex design. For the successful formation of our designed duplex, however, a “spacer” building

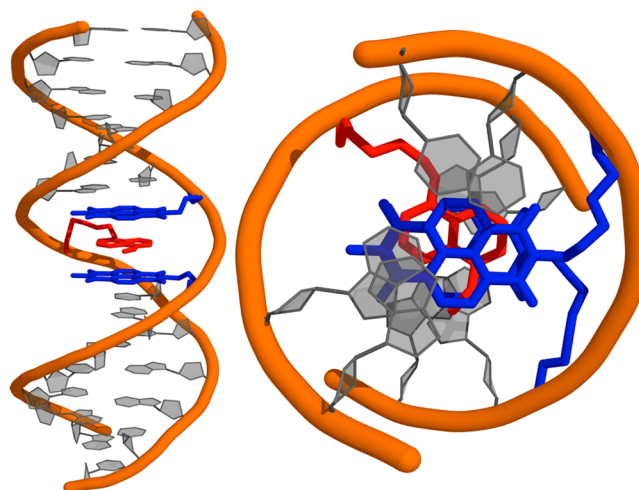


Figure 3. Model depicting the predicted NDI–DAN interaction: (left) side view; (right) top-down view. NDI and DAN are shown in blue and red, respectively.

block **3** based on (*S*)-1,2-propanediol (Figure 4) had to be placed across from each modified base to maintain proper backbone spacing.

Synthesis of the Phosphoramidites. The DAN phosphoramidite **1** was synthesized starting with the monomethylation of 1,5-dihydroxynaphthalene utilizing a stoichiometric amount of methyl iodide (Scheme 1). The product was further alkylated with 3-bromopropan-1-ol to yield alcohol **6**. Intermediate **6** was then reacted with (*R*)-(+)-glycidol through a regio- and enantiospecific epoxide opening mediated by DIBALH to give diol **7** in 29% yield with an enantiomeric excess of 99% (chiral HPLC).³⁷ Diol **7** was selectively protected on the primary hydroxyl group using 4,4'-dimethoxytrityl chloride and subsequently transformed into phosphoramidite **1** using standard conditions.³⁸

The synthesis of the NDI phosphoramidite **2** could not proceed by a similar epoxide-opening step because the imide carbonyls of NDI are sensitive to DIBALH, so an alternative

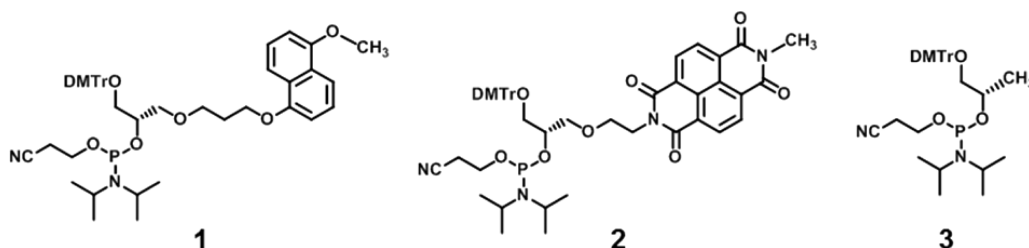
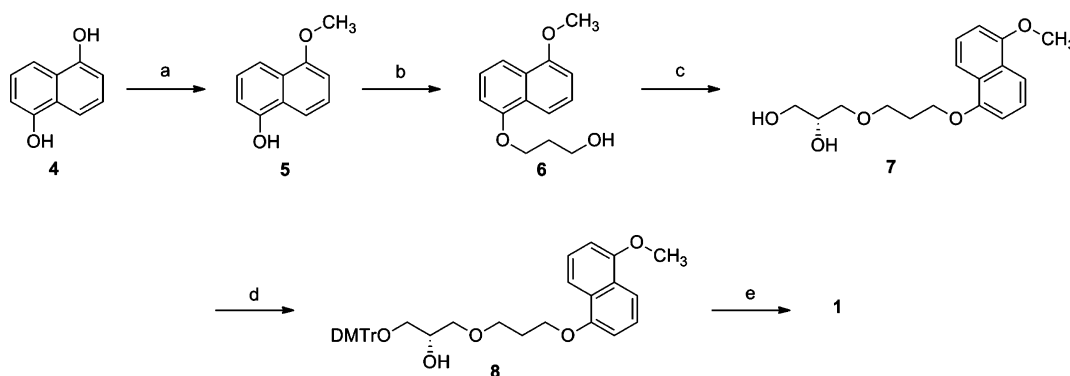


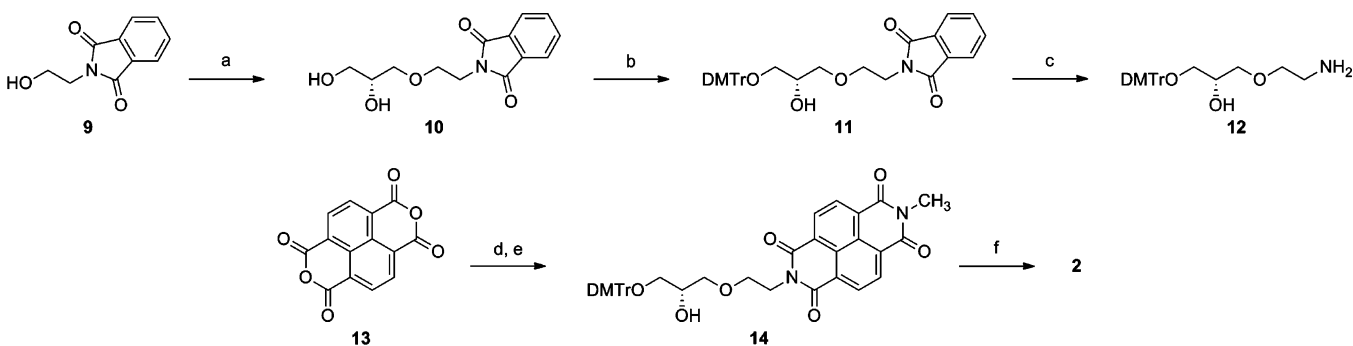
Figure 4. Structures of the phosphoramidite monomers.

Scheme 1^a



^aReagents and conditions: (a) MeI, K₂CO₃, MeCN, 82 °C, 37%; (b) 3-bromopropan-1-ol, K₂CO₃, MeCN, 82 °C, 75%; (c) (R)-(+)-glycidol, DIBALH, DCM, 0 °C → rt, 29%; (d) DMTrCl, DMAP, pyridine, rt, 35%; (e) (*i*-Pr)₂NP(Cl)OCH₂CH₂CN, DIPEA, DCM, rt, 73%.

Scheme 2^a



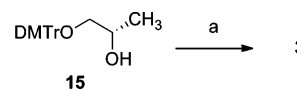
^aReagents and conditions: (a) (R)-(+)-glycidol, CsF, 130 °C, 24%; (b) DMTrCl, pyridine, rt, 89%; (c) MeNH₂, EtOH, 78 °C, 96%; (d) MeNH₂, DMF, μ wave, 75 °C → 140 °C, 83%; (e) 12, Et₃N, DMF, μ wave, 140 °C, 22%; (f) (*i*-Pr)₂NP(Cl)OCH₂CH₂CN, DIPEA, DCM, rt, 83%.

route was necessary (Scheme 2). This route involved phthalimide-protected ethanolamine **9**, which was used to open (R)-(+)-glycidol under mediation by CsF, giving diol **10** in 24% yield with an enantiomeric excess of 89% (chiral HPLC).³⁹ Because this was an initial study of the use of our new surrogate bases within this oligonucleotide system, the synthesis was carried on without separation of the enantiomers. Diol **10** was selectively protected on the primary hydroxyl group using 4,4'-dimethoxytrityl chloride under standard conditions.³⁸ The phthalimide protecting group was then removed using methylamine to yield free primary amine **12**. A microwave procedure was used to append the two primary amines to 1,4,5,8-tetracarboxylic acid dianhydride (**13**), first using methylamine to obtain the methyl monoimide and then using the free amino group of **12** to achieve the asymmetric NDI intermediate **14**.⁴⁰ Intermediate **14** was converted to the protected phosphoramidite **2** using standard conditions.³⁸

As shown in Scheme 3, the spacer phosphoramidite **3** was synthesized starting from compound **15** using conditions similar to those in previous syntheses.^{38,41}

Sequence Design. In order to investigate the DAN and NDI artificial DNA bases, a three-base-pair region was inserted into the interior of duplex **1**, a control DNA sequence of 12 base pairs (Figure 5). Four single-stranded 15-mer oligonucleotides with NDI and DAN modifications were designed to generate duplexes **5–8** as well as the oligonucleotides for the

Scheme 3^a



^aReagents and conditions: (a) (*i*-Pr)₂NP(Cl)OCH₂CH₂CN, DIPEA, DCM, rt, 79%.

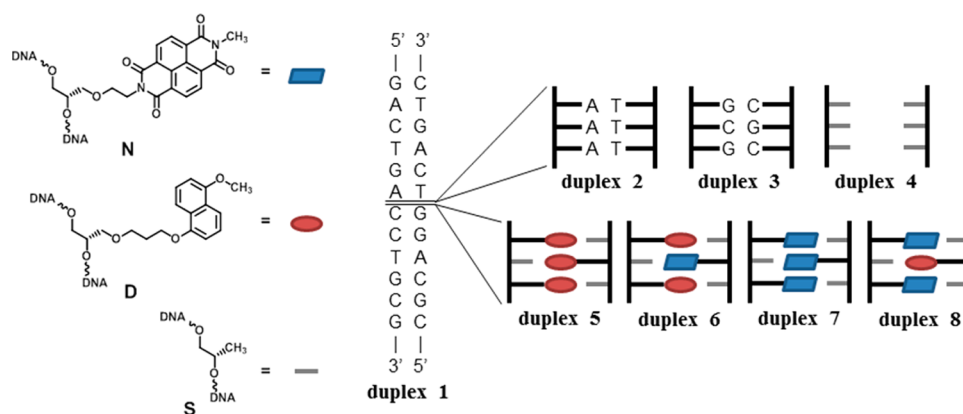


Figure 5. Modified DNA base surrogates and a cartoon representing the control DNA duplex 1 as well as the insertions of natural DNA bases (duplex 2 and duplex 3), spacer units (duplex 4), and the four NDI- and DAN-modified units (duplexes 5–8).

three control duplexes with three A–T, G–C, or spacer base pairs (duplexes 2–4, respectively). The control duplexes duplex 2 and duplex 3 both contain a deoxyribose backbone as a reference in order to compare our modified duplexes to natural DNA duplexes, noting that substituting a GNA backbone within a sequence of natural bases has been shown to destabilize the DNA duplex melting temperature.⁴² Duplex 5 was designed to examine the stability provided by stacking of three DAN units, while duplex 6 was designed to examine the stability provided by alternating DAN–NDI–DAN stacking. Duplex 7 was designed to examine the stability provided by stacking of three NDI units, while duplex 8 was designed to examine the stability provided by alternating NDI–DAN–NDI stacking. NDI is a known strong DNA intercalator^{43,44} and has been shown to have relatively high affinity for G-quadruplex DNA,^{45,46} and therefore, it is predicted to have greater association with natural DNA bases than DAN. This led to the prediction that duplex 8 (with two NDI–nucleobase contacts) would provide greater stability than duplex 6 (with two DAN–nucleobase contacts). For the same reason, and additionally because NDI is known to produce relatively stable self-stacks compared to DAN self-stacks, duplex 7 was predicted to provide significantly greater stability than duplex 5. Taken together, analysis of the relative stabilities of duplexes 1–8 allowed an assessment of the role that the electrostatic complementarity of DAN and NDI plays in stabilizing DNA duplexes and how such stability compares with those provided by natural A–T and G–C sequences.

Synthesis of Oligonucleotides. Oligonucleotides were synthesized on an automated nucleic acid synthesizer according to standard automated oligonucleotide synthesis protocols, except for those utilizing the building blocks 1, 2, and/or 3. These modified phosphoramidites were dissolved in a 3:1 CH₂Cl₂/CH₃CN solution to solubilize the monomers adequately. To avoid aminolysis of the imide functional group in NDI, oligonucleotides containing NDI were synthesized utilizing UltraMild synthesis and deprotection methods from Glen Research, which avoid the concentrated aqueous ammonia cleavage step. All of the oligonucleotides were characterized by HRMS-ESI (negative mode, CH₃CN/aqueous ammonium carbonate).

Thermal Denaturing Studies. Thermal denaturing studies were performed to quantify the influence of DAN and NDI stacking patterns on the duplex stability (Table 1). The highest melting temperature for any of the duplexes studied was seen

Table 1. *T_m* Data for the DNA Duplexes^a

Duplex	Sequence	<i>T_m</i> (°C)	Δ <i>T_m</i> (°C)
1	5' -GACTGACCTGCG-3' 3' -CTGACTGGACGC-5'	54	-
2	5' -GACTGA AAA CCTGCG-3' 3' -CTGACT TTT GGACGC-5'	58	4
3	5' -GACTGA GCG CCTGCG-3' 3' -CTGACT CGC GGACGC-5'	65	11
4	5' -GACTGA SSS CCTGCG-3' 3' -CTGACT SSS GGACGC-5'	24	-30
5	5' -GACTGA DSD CCTGCG-3' 3' -CTGACT SDS GGACGC-5'	42	-12
6	5' -GACTGA DSD CCTGCG-3' 3' -CTGACT SNS GGACGC-5'	52	-2
7	5' -GACTGA NSN CCTGCG-3' 3' -CTGACT SNS GGACGC-5'	53	-1
8	5' -GACTGA NSN CCTGCG-3' 3' -CTGACT SDS GGACGC-5'	57	3

^aDNA melting experiments were carried out at a duplex concentration of 1.5 μM (pH 7, 100 mM NaCl, 10 mM NaH₂PO₄, 0.1 mM EDTA).

for duplex 3 containing three G–C base pairs, which displayed a melting temperature 11 °C higher than that of the control duplex 1. The next most stable duplex was duplex 2 containing A–T base pairs, which exhibited a 4 °C increase in melting temperature compared with duplex 1. Duplex 4 containing three spacer units instead of any bases or aromatic units was by far the least stable duplex examined (its melting temperature was 30 °C lower than that of the control duplex 1), indicating that duplex 4 should probably be viewed as containing two hexamer duplexes that melt more or less independently.

As expected, the modified duplex with the highest melting temperature was duplex 8, which showed an increase in thermal stability of 3 °C compared with the control duplex 1. It should be noted that this melting temperature increase is comparable to that afforded by three A–T base pairs (duplex 2) but not as large as that seen with three G–C base pairs (duplex 3). Comparing duplex 7 with duplex 8 reveals that a 4 °C increase in melting temperature was afforded by changing the central NDI unit to a more electrostatically complementary DAN moiety in an NDI–DAN–NDI arrangement. Similarly,

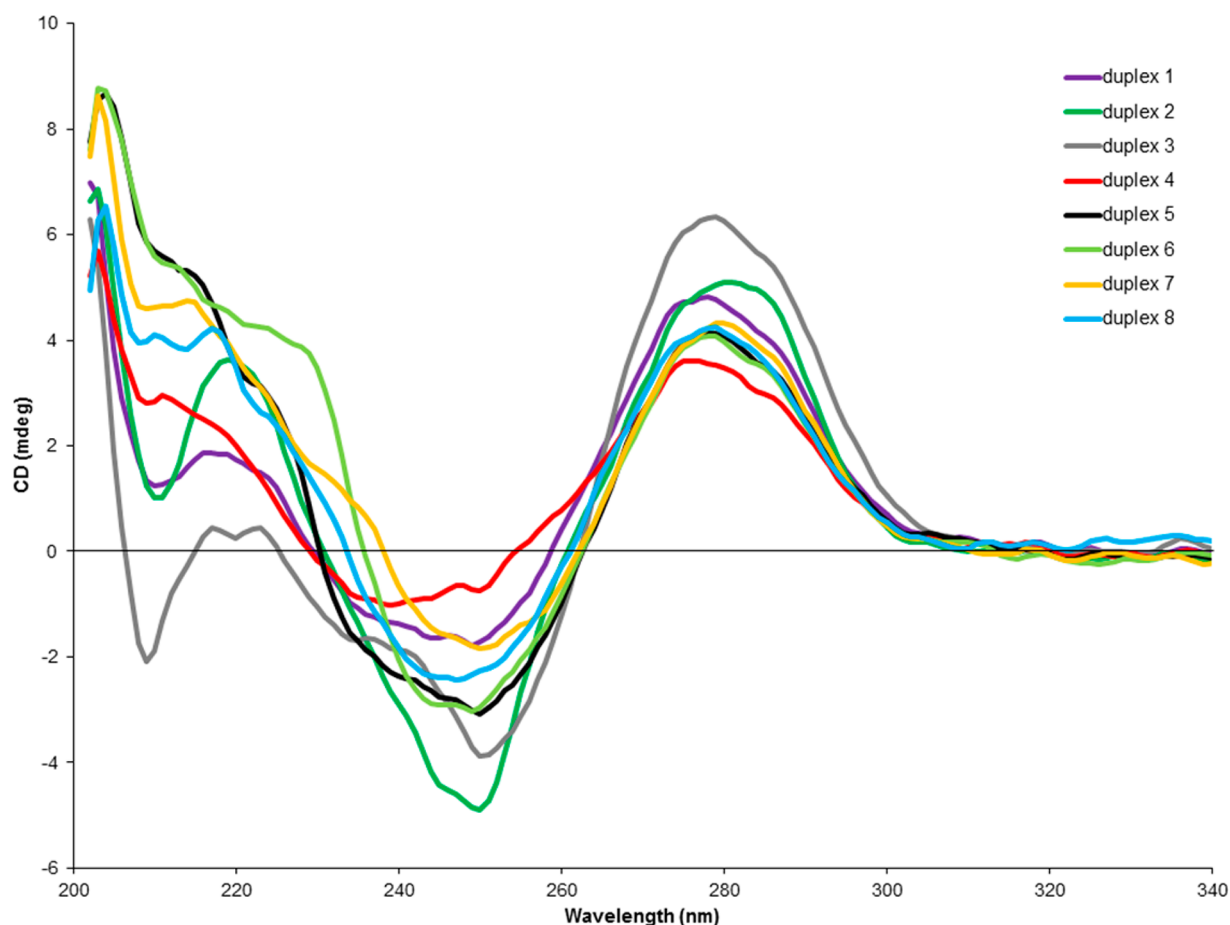


Figure 6. CD spectra of duplexes 1–8. All spectra were recorded at a duplex concentration of 1.5 μM (pH 7, 100 mM NaCl, 10 mM NaH_2PO_4 , 0.1 mM EDTA).

comparing **duplex 5** to **duplex 6** shows that a homo-DAN arrangement is also significantly less stabilizing than a DAN–NDI–DAN alternating duplex, in this case by 10 $^\circ\text{C}$. Finally, as expected, NDI–nucleobase interactions appear to be preferred over DAN–nucleobase interactions, as **duplex 8** exhibited a 5 $^\circ\text{C}$ higher melting point than **duplex 6**.

Circular Dichroism Spectra of the Duplexes. In order to investigate overall duplex structure, the duplexes were analyzed by CD spectroscopy (Figure 6). Each of the modified duplexes showed spectral features consistent with an overall B-form DNA topology, exhibiting a bisignate spectrum with a null occurring near $\lambda = 260$ nm. In addition, CD spectra at various temperatures ranging from 15 to 70 $^\circ\text{C}$ demonstrated behavior similar to that of the corresponding **duplex 1** CD spectra, which further supports its B-form structure. Although this is not a high-resolution technique, these results do rule out any substantial deviations from B-form structure in any of the duplexes. Unfortunately, little to no insight can be gained regarding the exact stacking topologies of the modified bases in **duplexes 4–8** from the CD spectra alone. Even at duplex concentrations of 10 μM , the relative concentration of NDI is too small to detect any significant CD signal, let alone changes within CD spectra, resulting from the NDI absorbance in the 300–400 nm range.

DISCUSSION

Taken together, our results indicate a strong preference for alternating NDI–DAN–NDI stacking relative to NDI–NDI–

NDI and especially DAN–DAN–DAN self-stacking within a DNA duplex. Upon comparison of the melting temperatures of **duplex 5** and **duplex 6**, an impressive 10 $^\circ\text{C}$ increase in melting temperature was observed upon replacement of the central DAN with NDI to create an alternating DAN–NDI–DAN arrangement. Consistent with this trend, comparing the melting temperatures of **duplex 7** and **duplex 8** shows that there was a 4 $^\circ\text{C}$ increase upon exchange of the central NDI to a DAN to create an alternating NDI–DAN–NDI arrangement. It is reasonable that the latter difference is less significant than the former because NDI is known to self-stack with relatively high stability, albeit in an offset stacking mode, while DAN self-stacking is not known to be favorable.²⁸ It thus appears that the known electrostatic complementarity between these units is stabilizing in the context of DNA duplexes, thereby exerting control over duplex specificity without the use of specific hydrogen-bonding patterns.

The NDI–DAN–NDI arrangement in **duplex 8** provided the most significant stability of any of the modified base sequences examined, as its melting temperature was 5 $^\circ\text{C}$ higher than that of the corresponding DAN–NDI–DAN **duplex 6**. This is as expected because NDI is a known DNA intercalator, so the two NDI–nucleobase interactions predicted to occur at either end of the NDI–DAN–NDI segment within **duplex 8** should be energetically favorable compared with the two DAN–nucleobase interactions predicted to occur at either end of the DAN–NDI–DAN segment within **duplex 6**.

Although no direct spectroscopic evidence for NDI and DAN stacking in any of the duplexes was obtained, the predictable differences in stabilities, consistent with the known preference for alternating NDI–DAN stacking, provides supporting evidence that especially in **duplex 8** the NDI and DAN units are stacked in, or close to, the preferred face-centered geometry. On the basis of CD analysis, we do know that the modified bases do not cause any significant deviations from the B-form structure of the entire duplex. Overall, these considerations indicate the design of non-natural base surrogates **1** and **2** was able to facilitate the desired NDI–DAN stacking within the context of a B-form DNA helix.

CONCLUSION

Two new DNA base surrogate building blocks based on DAN and NDI have been synthesized and incorporated into DNA oligonucleotide strands. In the most favorable arrangement, an NDI–DAN–NDI sequence in the middle of a DNA duplex was found to be approximately as stabilizing as three A–T base pairs. The results demonstrate that electrostatic complementarity between DAN and NDI can be used to drive the specificity and stability of DNA duplexes. Future work will explore how NDI and DAN units behave in alternate patterns within a DNA duplex, including their effect at the terminal positions of oligonucleotide duplexes as well as the thermodynamics of longer stretches of NDI and DAN within DNA.

EXPERIMENTAL SECTION

5-Methoxynaphthalen-1-ol (5). In a 100 mL round-bottom flask with a stir bar, 1,5-dihydroxynaphthalene (1.00 g, 6.2 mmol) was dissolved in 32 mL of acetonitrile. To the reaction mixture were added K_2CO_3 (0.95 g, 6.8 mmol) and CH_3I (0.39 mL, 6.2 mmol). A reflux condenser was fitted to the reaction flask, and the reaction vessel was purged with argon. The reaction mixture was stirred at reflux overnight and then cooled to room temperature, and the acetonitrile was removed in vacuo. The thick black reaction mixture was then dissolved in $CHCl_3$ and filtered through Celite. The filtrate was washed three times with saturated $NaHCO_3$ and three times with brine and then dried over Na_2SO_4 . The $CHCl_3$ was removed in vacuo, and the crude product was purified with silica gel column chromatography (2% acetone in $CHCl_3$) to give a tan solid (0.41 g, 2.4 mmol, 37% yield). Mp 128–132 °C. 1H NMR (400 MHz, $CDCl_3$, ppm) δ 7.85 (d, $J = 8.5$ Hz, 1H), 7.74 (d, $J = 8.5$ Hz, 1H), 7.40 (t, $J = 7.7$ Hz, 1H), 7.30 (t, $J = 7.5$ Hz, 1H), 6.85 (d, $J = 7.4$ Hz, 2H), 5.23 (s, 1H), 4.00 (s, 3H). ^{13}C NMR (400 MHz, $CDCl_3$, ppm) δ 155.3, 151.1, 126.9, 125.3, 125.1, 114.7, 113.6, 109.4, 104.4, 55.5. HRMS-ESI (m/z) calcd for $C_{11}H_{11}O_2^+$ [$M + H$] $^+$ 175.0754, found 175.0760.

3-((5-Methoxynaphthalen-1-yl)oxy)propan-1-ol (6). In a 250 mL three-neck round-bottom flask with a stir bar, **5** (1.47 g, 8.42 mmol) was dissolved in 84 mL of acetonitrile. To the reaction mixture were added K_2CO_3 (1.28 g, 9.27 mmol) and 3-bromopropan-1-ol (1.32 mL, 15.10 mmol). The flask was fitted with a condenser and septa and purged with argon. The reaction mixture was heated at reflux for 24 h and then cooled to room temperature, and the acetonitrile was removed in vacuo. The thick black reaction mixture was dissolved in CH_2Cl_2 and filtered through Celite. The CH_2Cl_2 was removed in vacuo, and the reaction mixture was purified by silica gel column chromatography (5% acetone in CH_2Cl_2) to give a light-tan solid (1.47 g, 6.33 mmol, 75% yield). Mp 100–102 °C. 1H NMR (400 MHz, $CDCl_3$, ppm) δ 7.83 (dd, $J = 14.0, 8.9$ Hz, 2H), 7.42–7.33 (m, 2H), 6.86 (t, $J = 7.7$ Hz, 2H), 4.27 (t, $J = 5.8$ Hz, 2H), 3.99 (s, 3H), 3.96 (t, $J = 6.0$ Hz, 2H), 2.18 (p, $J = 6.0$ Hz, 2H), 1.83 (s, 1H). ^{13}C NMR (400 MHz, $CDCl_3$, ppm) δ 155.2, 154.3, 126.6, 126.5, 125.2, 125.1, 114.3, 114.0, 105.5, 104.5, 65.6, 60.5, 55.5, 32.1. HRMS-ESI (m/z) calcd for $C_{14}H_{16}O_3^+$ [M] $^+$ 232.1099, found 232.1101.

(R)-3-(3-((5-Methoxynaphthalen-1-yl)oxy)propoxy)propane-1,2-diol (7). To a clean dry 50 mL round-bottom flask were added **6** (0.5211 g, 2.245 mmol) and CH_2Cl_2 (15 mL). The reaction mixture was cooled to 0 °C with an ice bath, and DIBALH (1.25 mL of a 1.5 M solution in toluene, 1.875 mmol) was added. The reaction mixture was taken off the ice, allowed to warm to room temperature, and stirred for 30 min, and then (R)-(+)-glycidol (0.1 mL, 1.506 mmol) was added dropwise. The reaction mixture was stirred for 72 h at room temperature. Potassium sodium tartrate (0.5525 g, 1.959 mmol) dissolved in a minimal amount of water was added, and the reaction mixture was stirred for 30 min and then extracted three times with ethyl acetate. The resulting organic layers were combined and washed with water and brine. The product mixture was then dried over Na_2SO_4 and concentrated in vacuo. The product was purified by silica gel column chromatography (4% methanol in CH_2Cl_2) to give a brown solid (0.133 g, 0.434 mmol, 29% yield). Mp 48–50 °C. 1H NMR (400 MHz, $CDCl_3$, ppm) δ 7.84 (d, $J = 8.3$ Hz, 2H), 7.36 (dd, $J = 14.5, 7.8$ Hz, 2H), 6.82 (d, $J = 7.6$ Hz, 2H), 4.16 (t, $J = 6.1$ Hz, 2H), 3.97 (s, 3H), 3.88–3.81 (m, 1H), 3.71 (t, $J = 6.3$ Hz, 2H), 3.65 (dd, $J = 11.5, 3.6$ Hz, 1H), 3.56 (dd, $J = 11.5, 6.0$ Hz, 1H), 3.49–3.46 (m, 2H), 3.25 (s, 2H), 2.15 (p, $J = 6.2$ Hz, 2H). ^{13}C NMR (400 MHz, $CDCl_3$, ppm) δ 155.1, 154.2, 126.5, 125.1, 114.1, 114.0, 105.4, 104.4, 72.2, 70.6, 68.2, 64.7, 63.9, 55.4, 29.4. HRMS-ESI (m/z) calcd for $C_{17}H_{22}NaO_5^+$ [$M + Na$] $^+$ 329.1359, found 329.1355. $[\alpha]_D^{22} -7.3$ (c 0.50, $CHCl_3$). 99% ee as determined by HPLC (Chiralcel ODH column, 0.46 cm I.D. \times 25 cm long; eluent, hexane/*i*-PrOH 95:5 v/v; flow rate, 1.0 mL/min; UV at 254 nm; room temperature; see the Supporting Information).

(S)-1-(Bis(4-methoxyphenyl)(phenyl)methoxy)-3-(3-((5-methoxynaphthalen-1-yl)oxy)propoxy)propan-2-ol (8). In a clean, dry 50 mL round-bottom flask, **7** (0.4012 g, 1.3096 mmol) and DMAP (0.0160 g, 0.131 mmol) were dissolved in pyridine (13.1 mL). The atmosphere was purged with argon, and the mixture was stirred. Next, 4,4'-dimethoxytrityl chloride (0.4508 g, 1.330 mmol) was slowly added to the reaction mixture. The mixture was stirred overnight, and the pyridine was then removed in vacuo. The product was purified by silica gel column chromatography (1:1 hexanes/ethyl acetate with 0.1% triethylamine) to yield a light-tan oil (0.2793 g, 0.459 mmol, 35% yield). 1H NMR (400 MHz, $CDCl_3$, ppm) δ 7.83 (d, $J = 8.0$ Hz, 2H), 7.42 (d, $J = 7.1$ Hz, 2H), 7.38–7.33 (m, 2H), 7.33–7.27 (m, 6H), 7.23–7.17 (m, 1H), 6.87–6.77 (m, 6H), 4.18 (t, $J = 6.1$ Hz, 2H), 3.99 (s, 3H), 3.98–3.93 (m, 1H), 3.76 (s, 6H), 3.75–3.71 (m, 2H), 3.56 (ddd, $J = 16.0, 9.7, 5.3$ Hz, 2H), 3.18 (dd, $J = 5.5, 2.9$ Hz, 2H), 2.42 (s, 1H), 2.17 (p, $J = 6.2$ Hz, 2H). ^{13}C NMR (400 MHz, $CDCl_3$, ppm) δ 155.2, 154.3, 126.6, 125.1, 114.2, 114.0, 105.4, 104.4, 72.4, 70.5, 68.3, 64.8, 64.0, 55.5, 53.4, 29.6. HRMS-ESI (m/z) calcd for $C_{38}H_{40}NaO_7^+$ [$M + Na$] $^+$ 631.2666, found 631.2670.

(S)-1-(Bis(4-methoxyphenyl)(phenyl)methoxy)-3-(3-((5-methoxynaphthalen-1-yl)oxy)propoxy)propan-2-yl (2-Cyanoethyl) *N,N*-Diisopropylphosphoramidite (1). In a dry 15 mL round-bottom flask, **8** (0.2793 g, 0.459 mmol) was dissolved in CH_2Cl_2 (8.2 mL), and *N,N*-diisopropylethylamine (0.51 mL, 2.963 mmol) was added. The reaction mixture was stirred and purged with argon, and 2-cyanoethyl *N,N*-diisopropylchlorophosphoramidite (0.2 mL, 0.918 mmol) was added dropwise. The reaction mixture was stirred for 3 h at room temperature, poured into saturated aq. $NaHCO_3$, washed three times with CH_2Cl_2 , and dried over Na_2SO_4 . The CH_2Cl_2 was removed in vacuo, and the product was purified by silica gel column chromatography (4:1 hexanes/ethyl acetate with 0.1% triethylamine) to yield a mixture of diastereomers as a faint-yellow oil (0.270 g, 0.334 mmol, 73% yield). 1H NMR (400 MHz, $CDCl_3$, ppm) δ 7.86 (t, $J = 7.5$ Hz, 2H), 7.52–7.44 (m, 2H), 7.41–7.17 (m, 11H), 6.88–6.75 (m, 6H), 4.18 (dt, $J = 17.1, 6.0$ Hz, 3H), 4.00 (s, 3H), 3.80 (s, 2H), 3.76 (s, 6H), 3.74–3.69 (m, 2H), 3.69–3.60 (m, 3H), 3.60–3.48 (m, 1H), 3.30 (dd, $J = 9.4, 4.4$ Hz, 1H), 3.26–3.19 (m, 1H), 3.19–3.12 (m, 1H), 2.57–2.35 (m, 2H), 2.16 (tt, $J = 12.4, 6.1$ Hz, 2H), 1.20 (d, $J = 6.8$ Hz, 6H), 1.16 (d, $J = 6.7$ Hz, 3H), 1.05 (d, $J = 6.7$ Hz, 3H). ^{13}C NMR (400 MHz, $CDCl_3$, ppm) δ 158.5, 158.3, 155.1, 154.3, 144.9, 139.4, 136.1, 136.0, 130.0, 129.0, 128.2, 128.1, 127.8, 127.7, 127.6, 127.0, 126.6, 126.5, 125.2, 125.0, 117.7, 117.6, 114.1, 114.0, 113.9,

113.1, 112.9, 105.3, 104.4, 104.3, 85.9, 85.8, 72.7, 72.5, 72.3, 72.1, 71.8, 67.9, 67.8, 64.8, 64.1, 63.9, 58.4, 58.2, 55.4, 55.1, 43.1, 43.0, 42.9, 29.7, 29.6, 24.6, 24.5, 24.4, 20.1, 20.0. ^{31}P NMR (400 MHz, CDCl_3 , ppm) δ 149.4, 149.3. HRMS-ESI (m/z) calcd for $\text{C}_{47}\text{H}_{58}\text{N}_2\text{O}_8\text{P}^+$ [$\text{M} + \text{H}$] $^+$ 809.3925, found 809.3930.

2-(2-Hydroxyethyl)isoindoline-1,3-dione (9). Compound **9** was synthesized according to a protocol previously reported in the literature.⁴⁷ Mp 118–120 °C. ^1H NMR (400 MHz, CDCl_3 , ppm) δ 7.85–7.77 (m, 2H), 7.73–7.66 (m, 2H), 3.91–3.79 (m, 4H), 2.67 (s, 1H). ^{13}C NMR (400 MHz, CDCl_3 , ppm) δ 168.8, 134.0, 131.9, 123.3, 60.8, 40.7. HRMS-ESI (m/z) calcd for $\text{C}_{10}\text{H}_{10}\text{NO}_3^+$ [$\text{M} + \text{H}$] $^+$ 192.0655, found 192.0659.

(R)-2-(2-(2,3-Dihydroxypropoxy)ethyl)isoindoline-1,3-dione (10). To a 50 mL round-bottom flask were added CsF (0.081 g, 0.053 mmol) and **9** (4.7 g, 24.6 mmol). The reaction mixture was purged with argon, stirred, heated to 135 °C, and stirred for 45 min, and then (R)-(+)-glycidol (1.48 mL, 22.3 mmol) was added dropwise. The mixture was stirred overnight, cooled to room temperature, and dissolved in 4% methanol in CH_2Cl_2 . The product was purified by silica gel column chromatography (4% methanol in CH_2Cl_2) to yield a white solid (1.25 g, 4.70 mmol, 24% yield). Mp 59–61 °C. ^1H NMR (400 MHz, CDCl_3 , ppm) δ 7.84–7.78 (m, 2H), 7.72–7.66 (m, 2H), 3.87 (t, $J = 5.5$ Hz, 2H), 3.77 (dt, $J = 9.7, 4.8$ Hz, 1H), 3.73–3.64 (m, 2H), 3.61 (dd, $J = 11.5, 4.1$ Hz, 1H), 3.58–3.49 (m, 3H), 3.30 (s, 1H), 2.83 (s, 1H). ^{13}C NMR (400 MHz, CDCl_3 , ppm) δ 168.5, 134.0, 131.8, 123.3, 72.4, 70.4, 68.7, 63.6, 37.4. HRMS-ESI (m/z) calcd for $\text{C}_{13}\text{H}_{16}\text{NO}_5^+$ [$\text{M} + \text{H}$] $^+$ 266.1023, found 266.1024. $[\alpha]_D^{24} -8.7$ (c 0.73, CHCl_3). 89% ee as determined by HPLC (Chiralcel ODH column, 0.46 cm I.D. \times 25 cm long; eluent, hexane/*i*-PrOH 95:5 v/v; flow rate, 1.0 mL/min; UV at 254 nm; room temperature; see the Supporting Information).

(S)-2-(2-(3-(Bis(4-methoxyphenyl)(phenyl)methoxy)-2-hydroxypropoxy)ethyl)isoindoline-1,3-dione (11). In a dry 15 mL round-bottom flask, **10** (0.3526 g, 1.33 mmol) was dissolved in pyridine (6 mL). The mixture was purged with argon and stirred, and then 4,4'-dimethoxytrityl chloride (0.5435 g, 1.604 mmol) was slowly added. The mixture was stirred for 4 h, and the pyridine was removed in vacuo. The product was purified by silica gel column chromatography (1:1 hexanes/ethyl acetate with 0.1% triethylamine) to yield an off-white oil (0.6715 g, 1.183 mmol, 89% yield). ^1H NMR (400 MHz, CDCl_3 , ppm) δ 7.82 (dd, $J = 5.4, 3.1$ Hz, 2H), 7.70 (dd, $J = 5.5, 3.0$ Hz, 2H), 7.41 (d, $J = 7.2$ Hz, 2H), 7.28 (dd, $J = 14.0, 8.4$ Hz, 6H), 7.19 (t, $J = 7.2$ Hz, 1H), 6.81 (d, $J = 8.9$ Hz, 4H), 3.95–3.90 (m, 1H), 3.88 (t, $J = 5.7$ Hz, 2H), 3.78 (s, 6H), 3.71 (td, $J = 5.8, 2.8$ Hz, 2H), 3.62 (dd, $J = 9.6, 3.8$ Hz, 1H), 3.53 (dd, $J = 9.6, 6.7$ Hz, 1H), 3.14 (qd, $J = 9.4, 5.6$ Hz, 2H), 2.65 (d, $J = 4.6$ Hz, 1H). ^{13}C NMR (400 MHz, CDCl_3 , ppm) δ 168.3, 158.3, 144.8, 135.9, 133.9, 131.9, 129.9, 128.0, 127.7, 126.7, 123.2, 113.0, 85.9, 72.5, 69.7, 68.3, 64.3, 55.1, 37.4. HRMS-ESI (m/z) calcd for $\text{C}_{34}\text{H}_{33}\text{NO}_7\text{Na}^+$ [$\text{M} + \text{Na}$] $^+$ 590.2149, found 590.2150.

(S)-1-(2-Aminoethoxy)-3-(bis(4-methoxyphenyl)(phenyl)methoxy)propan-2-ol (12). In a dry 250 mL round-bottom flask, **11** (1.0084 g, 1.7765 mmol) was dissolved in ethanol (15 mL), and CH_3NH_2 (33% in ethanol, 30 mL, 141 mmol) was added. The reaction flask was fitted with a condenser and purged with argon, and the reaction mixture was heated to reflux for 2.5 h. The mixture was cooled to room temperature, and the solvent was removed in vacuo. The product was purified by silica gel column chromatography (10% methanol in CH_2Cl_2 with 0.1% triethylamine) to yield an off-white oil (0.4859 g, 1.111 mmol, 96% yield). ^1H NMR (400 MHz, CDCl_3 , ppm) δ 7.43 (d, $J = 7.3$ Hz, 2H), 7.32 (d, $J = 8.8$ Hz, 4H), 7.25 (t, $J = 7.5$ Hz, 2H), 7.16 (t, $J = 7.3$ Hz, 1H), 6.80 (d, $J = 8.9$ Hz, 4H), 3.94 (td, $J = 9.2, 5.8$ Hz, 1H), 3.72 (s, 6H), 3.59 (dd, $J = 10.0, 3.3$ Hz, 1H), 3.53–3.41 (m, 3H), 3.30 (s, 2H), 3.15 (ddd, $J = 21.1, 9.3, 5.7$ Hz, 2H), 2.78 (t, $J = 5.0$ Hz, 2H). ^{13}C NMR (400 MHz, CDCl_3 , ppm) δ 158.2, 144.6, 135.8, 129.8, 127.9, 127.5, 126.5, 112.8, 85.7, 72.7, 72.0, 69.4, 64.3, 63.2, 54.9, 41.0. HRMS-ESI (m/z) calcd for $\text{C}_{26}\text{H}_{31}\text{NO}_5\text{Na}^+$ [$\text{M} + \text{Na}$] $^+$ 460.2094, found 460.2095.

(S)-2-(2-(3-(Bis(4-methoxyphenyl)(phenyl)methoxy)-2-hydroxypropoxy)ethyl)-7-methylbenzo[*l,mn*][3,8]-

phenanthroline-1,3,6,8(2H,7H)-tetraone (14). In a clean, dry two-neck round-bottom flask, 1,4,5,8-naphthalenetetracarboxylic dianhydride (2.04 g, 7.61 mmol) was suspended in DMF (40 mL), and CH_3NH_2 (2 M in THF, 3.75 mL, 7.5 mmol) was added. The reaction mixture was sonicated for 5 min and then stirred and heated under microwave irradiation in the open reaction vessel fitted with a reflux condenser at 75 °C for 5 min and then 140 °C for 5 min. The reaction temperature was monitored by an internal probe. The reaction vessel was cooled to room temperature, and the solvent was removed in vacuo. The dark-brown solid was suspended in acetone, and the suspension was added to vigorously stirring 1 N HCl. The product was filtered, washed with water, and dried overnight in vacuo to yield a tan solid that was not purified any further (1.74 g, 6.17 mmol, 83% crude yield). ^1H NMR (400 MHz, $\text{DMSO}-d_6$, ppm) δ 8.73–8.65 (m, 4H), 3.43 (s, 3H). HRMS-ESI (m/z) calcd for $\text{C}_{15}\text{H}_8\text{NO}_5^+$ [$\text{M} + \text{H}$] $^+$ 282.0397, found 282.0395.

In a clean oven-dried microwave reaction vessel, the resulting crude product (0.2031 g, 0.7222 mmol) and **12** (0.2420 g, 0.5531 mmol) were dissolved in DMF (5 mL), and triethylamine (0.08 mL) was added. The reaction vessel was sealed and sonicated for 5 min. The reaction mixture was stirred and heated under microwave irradiation at 140 °C for 5 min and then allowed to cool to room temperature. The solvent was removed in vacuo, and the product was purified by silica gel column chromatography (1% methanol in CH_2Cl_2 with 0.2% triethylamine) to yield a tan frothy solid (0.0834 g, 0.1191 mmol, 22% yield). ^1H NMR (400 MHz, CDCl_3 , ppm) δ 8.65 (d, $J = 1.0$ Hz, 4H), 7.39 (d, $J = 7.2$ Hz, 2H), 7.25 (dd, $J = 13.4, 8.2$ Hz, 6H), 7.16 (t, $J = 7.2$ Hz, 1H), 6.76 (d, $J = 8.7$ Hz, 4H), 4.42 (t, $J = 5.7$ Hz, 2H), 3.94–3.88 (m, 1H), 3.84 (td, $J = 5.7, 1.8$ Hz, 2H), 3.74 (s, 6H), 3.67 (dd, $J = 9.6, 3.8$ Hz, 1H), 3.60 (dd, $J = 9.6, 6.6$ Hz, 1H), 3.56 (s, 3H), 3.18–3.08 (m, 2H), 2.73 (d, $J = 4.2$ Hz, 1H). ^{13}C NMR (400 MHz, CDCl_3 , ppm) δ 162.8, 158.4, 144.8, 136.0, 131.0, 130.9, 130.0, 128.1, 127.8, 126.7, 126.5, 126.4, 126.3, 113.0, 86.0, 72.7, 69.9, 68.2, 64.4, 55.2, 39.8, 27.4. HRMS-ESI (m/z) calcd for $\text{C}_{41}\text{H}_{36}\text{N}_2\text{O}_9\text{Na}^+$ [$\text{M} + \text{Na}$] $^+$ 723.2313, found 723.2317.

(S)-1-(Bis(4-methoxyphenyl)(phenyl)methoxy)-3-(2-(7-methyl-1,3,6,8-tetraoxo-7,8-dihydrobenzo[*l,mn*][3,8]phenanthroline-2(1H,3H,6H)-yl)ethoxy)propan-2-yl (2-Cyanoethyl) *N,N*-Diisopropylphosphoramidite (2). In a dry 5 mL round-bottom flask, **11** (0.0565 g, 0.0806 mmol) was dissolved in CH_2Cl_2 (1.5 mL), and *N,N*-diisopropylethylamine (0.09 mL, 0.517 mmol) was added. The reaction mixture was stirred and purged with argon, and 2-cyanoethyl *N,N*-diisopropylchlorophosphoramidite (0.05 mL, 0.2241 mmol) was added dropwise. The reaction mixture was stirred for 2 h at room temperature, poured into saturated aq. NaHCO_3 , washed three times with CH_2Cl_2 , and dried over Na_2SO_4 . The CH_2Cl_2 was removed in vacuo, and the product was purified by silica gel column chromatography (1:1 hexanes/ethyl acetate with 0.1% triethylamine) to yield a mixture of diastereomers as a faint-yellow oil (0.0605 g, 0.0671 mmol, 83% yield). ^1H NMR (400 MHz, CDCl_3 , ppm) δ 8.72–8.56 (m, 4H), 7.40 (t, $J = 7.9$ Hz, 2H), 7.31–7.19 (m, 6H), 7.15 (dd, $J = 14.0, 7.1$ Hz, 1H), 6.82–6.68 (m, 4H), 4.48–4.33 (m, 2H), 4.14–4.02 (m, 1H), 3.90–3.76 (m, 4H), 3.74 (d, $J = 3.6$ Hz, 6H), 3.71–3.62 (m, 3H), 3.56 (s, 3H), 3.51–3.42 (m, 1H), 3.23 (dd, $J = 9.6, 4.6$ Hz, 1H), 3.20–3.11 (m, 1H), 3.04 (dd, $J = 9.3, 6.4$ Hz, 1H), 2.64 (tq, $J = 7.6, 3.7$ Hz, 1H), 2.49–2.32 (m, 1H), 1.12 (dd, $J = 6.7, 3.8$ Hz, 6H), 1.08 (d, $J = 6.8$ Hz, 3H), 0.96 (d, $J = 6.8$ Hz, 3H). ^{13}C NMR (400 MHz, CDCl_3 , ppm) δ 162.8, 162.5, 158.2, 144.8, 136.0, 135.9, 130.8, 130.7, 129.9, 129.8, 128.1, 128.0, 127.5, 126.5, 126.4, 126.3, 126.2, 117.9, 117.6, 112.8, 85.8, 72.6, 72.5, 72.2, 72.0, 71.9, 67.8, 64.0, 63.8, 58.4, 58.3, 58.2, 58.1, 55.0, 43.0, 42.9, 42.8, 39.7, 39.5, 27.2, 24.5, 24.4, 24.3, 24.2, 20.2, 20.1, 20.0. ^{31}P NMR (400 MHz, CDCl_3 , ppm) δ 149.5, 149.1. HRMS-ESI (m/z) calcd for $\text{C}_{50}\text{H}_{53}\text{N}_4\text{O}_{10}\text{PNa}^+$ [$\text{M} + \text{Na}$] $^+$ 923.3392, found 923.3375.

(S)-1-(Bis(4-methoxyphenyl)(phenyl)methoxy)propan-2-ol (15). Compound **15** was synthesized according to a protocol previously reported in the literature.⁴¹ ^1H NMR (400 MHz, CDCl_3 , ppm) δ 7.44 (d, $J = 7.1$ Hz, 2H), 7.31 (dd, $J = 15.4, 8.4$ Hz, 6H), 7.25–7.16 (m, 1H), 6.84 (d, $J = 9.0$ Hz, 4H), 4.03–3.93 (m, 1H), 3.80 (s, 6H), 3.13 (dd, $J = 9.2, 3.4$ Hz, 1H), 3.00 (dd, $J = 9.2, 7.9$ Hz, 1H),

2.42 (s, 1H), 1.11 (d, $J = 6.4$ Hz, 3H). ^{13}C NMR (400 MHz, CDCl_3 , ppm) δ 158.4, 144.8, 136.0, 130.0, 129.1, 128.1, 127.8, 126.8, 113.1, 86.0, 68.8, 67.1, 55.2, 18.9. HRMS-ESI (m/z) calcd for $\text{C}_{24}\text{H}_{26}\text{O}_4\text{Na}^+$ [$\text{M} + \text{Na}$] $^+$ 401.1723, found 401.1727.

(S)-1-(Bis(4-methoxyphenyl)(phenyl)methoxy)propan-2-yl (2-Cyanoethyl) *N,N*-Diisopropylphosphoramidite (3). In a dry 50 mL round-bottom flask, **15** (0.2608 g, 0.6891 mmol) was dissolved in CH_2Cl_2 (12.3 mL), and *N,N*-diisopropylethylamine (0.77 mL, 4.4102 mmol) was added. The reaction mixture was stirred and purged with argon, and 2-cyanoethyl *N,N*-diisopropylchlorophosphoramidite (0.31 mL, 1.3897 mmol) was added dropwise. The reaction mixture was stirred for 3.5 h at room temperature, poured into saturated aq. NaHCO_3 , washed three times with CH_2Cl_2 , and dried over Na_2SO_4 . The CH_2Cl_2 was removed in vacuo, and the product was purified by silica gel column chromatography (1:4 hexanes/ethyl acetate with 0.1% triethylamine) to yield a mixture of diastereomers as a faint-yellow oil (0.3146 g, 0.5437 mmol, 79% yield). ^1H NMR (400 MHz, CDCl_3 , ppm) δ 7.48 (d, $J = 8.3$ Hz, 2H), 7.36 (dd, $J = 8.9, 3.7$ Hz, 4H), 7.28 (dd, $J = 14.6, 7.4$ Hz, 2H), 7.20 (dd, $J = 14.7, 8.6$ Hz, 1H), 6.83 (t, $J = 8.5$ Hz, 4H), 4.21–4.04 (m, 1H), 3.91–3.82 (m, 1H), 3.79 (d, $J = 3.5$ Hz, 6H), 3.77–3.72 (m, 1H), 3.70–3.51 (m, 2H), 3.22–3.14 (m, 1H), 3.02 (dd, $J = 9.4, 4.6$ Hz, 1H), 2.91 (dd, $J = 9.0, 5.7$ Hz, 1H), 2.62 (t, $J = 6.5$ Hz, 1H), 2.56–2.41 (m, 1H), 1.28 (t, $J = 5.3$ Hz, 3H), 1.24–1.16 (m, 9H), 1.11 (d, $J = 6.8$ Hz, 3H). ^{13}C NMR (400 MHz, CDCl_3 , ppm) δ 158.3, 145.0, 136.3, 136.2, 130.1, 130.0, 129.1, 128.2, 127.7, 127.6, 126.6, 126.5, 117.7, 113.1, 112.9, 85.8, 85.7, 70.0, 69.8, 68.0, 67.8, 67.8, 58.5, 58.3, 58.1, 57.9, 55.1, 43.0, 42.9, 24.7, 24.6, 24.5, 24.4, 20.4, 20.3, 20.2, 19.7, 19.6. ^{31}P NMR (400 MHz, CDCl_3 , ppm) δ 147.7, 147.4. HRMS-ESI (m/z) calcd for $\text{C}_{33}\text{H}_{44}\text{N}_2\text{O}_5\text{P}^+$ [$\text{M} + \text{H}$] $^+$ 579.2982, found 579.2977.

Oligonucleotide Synthesis. Unmodified oligonucleotides were synthesized on an automated nucleic acid synthesizer using a standard protocol for 2-cyanoethyl phosphoramidites (0.067 M) on a Glen UnySupport expedite format column on a 1 μmol scale. Because of their poor solubility in CH_3CN , all of the modified-base phosphoramidites were diluted with 3:1 $\text{CH}_2\text{Cl}_2/\text{CH}_3\text{CN}$. The oligonucleotides were synthesized using a trityl-on synthesis and cleaved from the resin with 1 mL of concentrated aqueous ammonia at room temperature for 12–24 h. The cleaved oligonucleotides were diluted with 1 mL of NaCl solution (100 mg/mL) and then semipurified by application to a Glen Pak purification column.

To avoid aminolysis, oligonucleotides containing NDI were synthesized utilizing UltraMild synthesis and deprotection methods from Glen Research. UltraMild-compatible phosphoramidites (Pac-dA-CE, Ac-dC-CE, and iPr-Pac-dG-CD phosphoramidites) and the Universal Support III expedite format column on a 1 μmol scale were used. The oligonucleotides were cleaved from the resin using the UltraMild deprotection solution (0.05 M K_2CO_3 in methanol) for 12 h and then diluted with 1 mL of 0.1 M TEAA, neutralized with 6 μL of glacial acetic acid, and lyophilized. The resulting dried crude trityl-on oligonucleotides were dissolved in 2 mL of 0.1 M TEAA and then applied directly on a Glen Pak purification column. The standard protocol for trityl-on oligonucleotides was used for the Glen Pak purification columns to afford the semipurified detritylated oligonucleotides. All of the semipurified oligonucleotides were last purified by reversed-phase HPLC using a C18 peptide semipreparatory reversed-phase column with 0.1 M aqueous TEAA (pH 7) and CH_3CN as the eluent. All of the oligonucleotides were characterized by HRMS-ESI (negative mode, $\text{CH}_3\text{CN}/\text{aqueous ammonium carbonate}$) (see the Supporting Information).

Thermal Denaturing Studies. Samples of each oligonucleotide strand were prepared at a concentration of 3 μM in phosphate buffer (pH 7, 100 mM NaCl, 10 mM NaH_2PO_4 , 0.1 mM EDTA). The oligonucleotide concentrations were quantified by measuring the absorbance at 260 nm. The corresponding molar extinction coefficients were calculated by summing up the individual extinction coefficients for all of the bases in the sequence. The molar extinction coefficients for dA, dG, dT, dC, **1**, **2**, and **3** at 260 nm were taken as 15 400, 11 500, 8700, 7400, 2504, 1955, and 0 $\text{M}^{-1} \text{cm}^{-1}$, respectively. Because the contents of the non-natural DNA base analogues were

small compared with the amounts of naturally occurring DNA bases, it is unlikely that this approximation caused any major discrepancies in DNA concentration. The melting studies were performed in a Teflon-stoppered 1 cm path length quartz cell on a UV–vis spectrophotometer equipped with a thermoprogrammer. Each melting temperature run involved combining 0.5 mL of complementary strand samples to obtain 1.5 μM duplex in solution. The samples were initially heated to 85 $^\circ\text{C}$ for 5 min and then cooled from 85 to 70 $^\circ\text{C}$ at a rate of 1 $^\circ\text{C}/\text{min}$ and then from 70 to 5 $^\circ\text{C}$ at a rate of 0.5 $^\circ\text{C}/\text{min}$. The absorbance at 260 nm was monitored. Two runs of these experiments were carried out per sample and averaged.

CD Spectroscopy. CD spectra were recorded on a circular spectropolarimeter, and all of the spectra were measured in a 1 cm path length quartz cell. Samples were prepared from UV melting temperature studies (1.5 μM in duplex concentration) in a phosphate buffer (pH 7, 100 mM NaCl, 10 mM NaH_2PO_4 , 0.1 mM EDTA). Samples were initially heated to 85 $^\circ\text{C}$ for 5 min and allowed to cool to room temperature for 45 min before the CD data were collected. The experiments were carried out at 25 $^\circ\text{C}$.

■ ASSOCIATED CONTENT

📄 Supporting Information

General procedures for synthetic methods; chiral HPLC chromatograms of **7** and **10**; ^1H , ^{13}C , and ^{31}P NMR spectra of synthesized compounds; molecular masses of individual oligonucleotides measured by ESI high-resolution mass spectrometry; HPLC chromatograms of modified oligonucleotides; methods for determining extinction coefficients of **1** and **2**; and UV melting temperature curves. This material is available free of charge via the Internet at <http://pubs.acs.org>.

■ AUTHOR INFORMATION

✉ Corresponding Author

*E-mail: iversonb@austin.utexas.edu.

Notes

The authors declare no competing financial interest.

■ ACKNOWLEDGMENTS

We thank Dr. Sean Kerwin for access to a UV–vis spectrophotometer and Dr. Andrew Ellington for access to the automated DNA synthesizer. This work was supported by the Robert A. Welch Foundation (F1188) and the National Institutes of Health (GM-069647).

■ REFERENCES

- (1) Malinovskii, V. L.; Wenger, D.; Häner, R. *Chem. Soc. Rev.* **2010**, *39*, 410–422.
- (2) Bandy, T. J.; Brewer, A.; Burns, J. R.; Marth, G.; Nguyen, T.; Stulz, E. *Chem. Soc. Rev.* **2011**, *40*, 138–148.
- (3) Chiba, J.; Inouye, M. *Chem. Biodiversity* **2010**, *7*, 259–282.
- (4) Cantor, C. R.; Schimmel, P. R. *Biophysical Chemistry Part III: The Behavior of Biological Macromolecules*; W.H. Freeman: New York, 1980; Vol. 2, pp 1109–1181.
- (5) Saenger, W. *Principles of Nucleic Acid Structure*; Springer: New York, 1984.
- (6) Teo, Y. N.; Kool, E. T. *Bioconjugate Chem.* **2009**, *20*, 2371–2380.
- (7) Grigorenko, N. A.; Leumann, C. J. *Chem. Commun.* **2008**, 5417–5419.
- (8) Roethlisberger, P.; Wojciechowski, F.; Leumann, C. J. *Chem.—Eur. J.* **2013**, *19*, 11518–11521.
- (9) Wagenknecht, H.-A. *Angew. Chem., Int. Ed.* **2009**, *48*, 2838–2841.
- (10) Zheng, Y.; Long, H.; Schatz, G. C.; Lewis, F. D. *Chem. Commun.* **2005**, 4795–4797.
- (11) Wang, W.; Wan, W.; Zhou, H.-H.; Niu, S.; Li, A. D. Q. *J. Am. Chem. Soc.* **2003**, *125*, 5248–5249.

- (12) Endo, M.; Shiroyama, T.; Fujitsuka, M.; Majima, T. *J. Org. Chem.* **2005**, *70*, 7468–7472.
- (13) Endo, M.; Fujitsuka, M.; Majima, T. *J. Org. Chem.* **2008**, *73*, 1106–1112.
- (14) Wojciechowski, F.; Leumann, C. J. *Chem. Soc. Rev.* **2011**, *40*, 5669–5679.
- (15) Schweitzer, B. A.; Kool, E. T. *J. Am. Chem. Soc.* **1995**, *117*, 1863–1872.
- (16) Leconte, A. M.; Hwang, G. T.; Matsuda, S.; Capek, P.; Hari, Y.; Romesberg, F. E. *J. Am. Chem. Soc.* **2008**, *130*, 2336–2343.
- (17) Yamashige, R.; Kimoto, M.; Takezawa, Y.; Sato, A.; Mitsui, T.; Yokoyama, S.; Hirao, I. *Nucleic Acids Res.* **2012**, *40*, 2793–2806.
- (18) Switzer, C.; Moroney, S. E.; Benner, S. A. *J. Am. Chem. Soc.* **1989**, *111*, 8322–8323.
- (19) Piccirilli, J. A.; Krauch, T.; Moroney, S. E.; Benner, S. A. *Nature* **1990**, *343*, 33–37.
- (20) Schweitzer, B. A.; Kool, E. T. *J. Org. Chem.* **1994**, *59*, 7238–7242.
- (21) Khakshoor, O.; Wheeler, S. E.; Houk, K. N.; Kool, E. T. *J. Am. Chem. Soc.* **2012**, *134*, 3154–3163.
- (22) Brotschi, C.; Mathis, G.; Leumann, C. J. *Chem.—Eur. J.* **2005**, *11*, 1911–1923.
- (23) Lokey, R. S.; Iverson, B. L. *Nature* **1995**, *375*, 303–305.
- (24) Zych, A. J.; Iverson, B. L. *J. Am. Chem. Soc.* **2000**, *122*, 8898–8909.
- (25) Gabriel, G. J.; Iverson, B. L. *J. Am. Chem. Soc.* **2002**, *124*, 15174–15175.
- (26) Talukdar, P.; Bollot, G.; Mareda, J.; Sakai, N.; Matile, S. *J. Am. Chem. Soc.* **2005**, *127*, 6528–6529.
- (27) Das, A.; Molla, M. R.; Maity, B.; Koley, D.; Ghosh, S. *Chem.—Eur. J.* **2012**, *18*, 9849–9859.
- (28) Cubberley, M. S.; Iverson, B. L. *J. Am. Chem. Soc.* **2001**, *123*, 7560–7563.
- (29) Wheeler, S. E. *J. Am. Chem. Soc.* **2011**, *133*, 10262–10274.
- (30) Martinez, C. R.; Iverson, B. L. *Chem. Sci.* **2012**, *3*, 2191–2201.
- (31) Liu, L.; Guo, Q.-X. *Chem. Rev.* **2001**, *101*, 673–696.
- (32) Reczek, J. J.; Villazor, K. R.; Lynch, V.; Swager, T. M.; Iverson, B. L. *J. Am. Chem. Soc.* **2006**, *128*, 7995–8002.
- (33) Alvey, P. M.; Reczek, J. J.; Lynch, V.; Iverson, B. L. *J. Org. Chem.* **2010**, *75*, 7682–7690.
- (34) Johnson, A. T.; Schlegel, M. K.; Meggers, E.; Essen, L.-O.; Wiest, O. *J. Org. Chem.* **2011**, *76*, 7964–7974.
- (35) Schlegel, M. K.; Essen, L.-O.; Meggers, E. *J. Am. Chem. Soc.* **2008**, *130*, 8158–8159.
- (36) Schlegel, M. K.; Xie, X.; Zhang, L.; Meggers, E. *Angew. Chem., Int. Ed.* **2009**, *48*, 960–963.
- (37) Erukulla, R. K.; Locke, D. C.; Bittman, R.; Byun, H.-S. *J. Chem. Soc., Perkin Trans. 1* **1995**, 2199–2200.
- (38) Zhang, L.; Peritz, A. E.; Carroll, P. J.; Meggers, E. *Synthesis* **2006**, 645–653.
- (39) Kitaori, K.; Furukawa, Y.; Yoshimoto, H.; Otera, J. *Tetrahedron* **1999**, *55*, 14381–14390.
- (40) Tambara, K.; Ponnuswamy, N.; Hennrich, G.; Pantos, G. D. *J. Org. Chem.* **2011**, *76*, 3338–3347.
- (41) Fathi, R.; Rudolph, M. J.; Gentles, R. G.; Patel, R.; MacMillan, E. W.; Reitman, M. S.; Pelham, D.; Cook, A. F. *J. Org. Chem.* **1996**, *61*, 5600–5609.
- (42) Schlegel, M. K.; Peritz, A. E.; Kittigowittana, K.; Zhang, L.; Meggers, E. *ChemBioChem* **2007**, *8*, 927–932.
- (43) Yen, S. F.; Gabbay, E. J.; Wilson, W. D. *Biochemistry* **1982**, *21*, 2070–2076.
- (44) Rhoden Smith, A.; Iverson, B. L. *J. Am. Chem. Soc.* **2013**, *135*, 12783–12789.
- (45) Cuenca, F.; Greciano, O.; Gunaratnam, M.; Haider, S.; Munnur, D.; Nanjunda, R.; Wilson, W. D.; Neidle, S. *Bioorg. Med. Chem. Lett.* **2008**, *18*, 1668–1673.
- (46) Di Antonio, M.; Doria, F.; Richter, S. N.; Bertipaglia, C.; Mella, M.; Sissi, C.; Palumbo, M.; Freccero, M. *J. Am. Chem. Soc.* **2009**, *131*, 13132–13141.
- (47) Billman, J. H.; Parker, E. E. *J. Am. Chem. Soc.* **1943**, *65*, 761–762.